University of Dayton
eCommons

Mechanical and Aerospace Engineering Faculty Publications

Department of Mechanical and Aerospace Engineering

1-1998

A Study of the Fundamental Operations of a Capillary Driven Heat Transfer Device in Both Normal and Low Gravity Part 1-Liquid Slug Formation in Low Gravity

Jeffrey S. Allen
NASA Glenn Research Center

Kevin P. Hallinan
University of Dayton, khallinan1@udayton.edu

Jack Lekan
NASA Lewis Research Center

Follow this and additional works at: https://ecommons.udayton.edu/mee_fac_pub

 Part of the Mechanical Engineering Commons

eCommons Citation

Allen, Jeffrey S.; Hallinan, Kevin P.; and Lekan, Jack, "A Study of the Fundamental Operations of a Capillary Driven Heat Transfer Device in Both Normal and Low Gravity Part 1-Liquid Slug Formation in Low Gravity" (1998). *Mechanical and Aerospace Engineering Faculty Publications*. 38.
https://ecommons.udayton.edu/mee_fac_pub/38

This Conference Paper is brought to you for free and open access by the Department of Mechanical and Aerospace Engineering at eCommons. It has been accepted for inclusion in Mechanical and Aerospace Engineering Faculty Publications by an authorized administrator of eCommons. For more information, please contact frice1@udayton.edu, mschlangen1@udayton.edu.

A STUDY OF THE FUNDAMENTAL OPERATIONS OF A CAPILLARY DRIVEN HEAT TRANSFER DEVICE IN BOTH NORMAL AND LOW GRAVITY

PART 1. LIQUID SLUG FORMATION IN LOW GRAVITY

Jeffrey S. Allen
University of Dayton
c/o NASA Lewis Research Center
21000 Brookpark Road
Cleveland, Ohio 44135
216-433-3087

Kevin Hallinan
Department of Mechanical
and Aerospace Engineering
University of Dayton
300 College Park
Dayton, Ohio 45469
937-229-2875

Jack Lekan
Mail Stop 500-216
NASA Lewis Research Center
21000 Brookpark Road
Cleveland, Ohio 44135
216-433-3459

Abstract

Research has been conducted to observe the operation of a capillary pumped loop (CPL) in both normal and low gravity environments in order to ascertain the causes of device failure. The failures of capillary pumped heat transport devices in low gravity; specifically; evaporator dryout, are not understood and the available data for analyzing the failures is incomplete. To observe failure in these devices an idealized experimental CPL was configured for testing in both a normal-gravity and a low-gravity environment. The experimental test loop was constructed completely of Pyrex tubing to allow for visualization of system operations. Heat was added to the liquid on the evaporator side of the loop using resistance heaters and removed on the condenser side via forced convection of ambient air. A video camera was used to record the behavior of both the condenser and the evaporator menisci simultaneously. Low-gravity experiments were performed during the Microgravity Science Laboratory (MSL-1) mission performed onboard the Space Shuttle Columbia in July of 1997. During the MSL-1 mission, a failure mechanism, heretofore unreported, was observed. In every experiment performed a slug of liquid would form at the transition from a bend to a straight run in the vapor line. Ultimately, this liquid slug prevents the flow of vapor to the condenser causing the condenser to eventually dryout. After condenser dryout, liquid is no longer fed into the evaporator and it, too, will dry out resulting in device failure. An analysis is presented to illustrate the inevitable formation of such liquid slugs in CPL devices in low gravity.

INTRODUCTION

Capillary pumped loops (CPL's) are used to transfer heat from one location to another using the latent heat of the working fluid. The basic CPL operation is illustrated in Figure 1. Heat is added to a porous wick where the liquid evaporates and the vapor recondenses at the cold end of the loop. The liquid is then driven back to the evaporator by the capillary pressure difference between the condenser meniscus and the menisci in the porous media in the evaporator. The advantages of CPL's are that they are entirely passive, requiring no power, and can transfer heat over distances as large as 10 or more meters. These features are very desirable for spacecraft operations. Unfortunately, CPL's have proven to be unreliable in low-gravity operations.

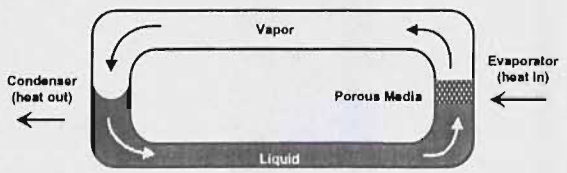

FIGURE 1. Schematic of Operations in a Capillary Pumped Loop (CPL)

Previous research of high power capillary pumped loops has revealed operating characteristics which at times fall well-below design predictions of the heat transport capability. Richter and Gottschlich (1994) have observed that design predictions for low temperatuer CPL's significantly over estimate the experimentally realized heat transport. In the experimental work of Ku, Kroliczek, McCabe, and Benner (1988) pressure oscillations across the evaporators with a magnitude as large as 700 Pa (0.1 psi) were observed. Later, Ku (1995), reported that when these pressure oscillations are present, the maximum heat transport can be as little as 10% of the design value. Finally, the CPL GAS can, CAPL, CAPL-2, View-CPL, and TPF low-gravity technology demonstration experiments, all based out of NASA Goddard Space Flight Center, have reported difficulty in start-up of capillary pumped loops.

CP420, *Space Technology and Applications International Forum-1998*
edited by Mohamed S. El-Genk

DOE CONF-980103 © 1998 The American Institute of Physics 1-56396-747-2/98/$10.00

The Capillary-driven Heat Transfer (CHT) experiment was conceived to study the fundamental fluid physics phenomena thought to be responsible for the failure of CPL's in low-gravity operations.

EXPERIMENT

The principle component of the Capillary-driven Heat Transfer (CHT) experiment is a glass test loop which is illustrated in Figure 2. Within the loop is a three-way valve; referred to as the control valve. The control valve directs liquid flow from the reservoir into the condenser leg and/or the evaporator leg of the test loop. During the experiment, the control valve allows for liquid flow from the condenser leg to the evaporator leg while isolating the reservoir. The reservoir is constructed from a 10cc gas tight syringe with a screw type plunger which allows for repeatable fills. The liquid leg of the test loop is constructed of Pyrex capillary tubing. The vapor leg of the test loop is constructed from 10mm diameter Pyrex tubing. Two conical transition sections connect the vapor leg to the liquid leg. The conical sections are designed to be capillary traps in low gravity so as to preferentially locate the evaporator meniscus. A capillary pumping potential is established by the difference between the pressure drop across the condenser meniscus in the 10mm tube and the pressure drop across the evaporator meniscus in the capillary tube (1mm or 4mm in diameter). The difference in the condenser and evaporator diameters allows for the capillary pumping potential to be maintained even with a large temperature difference between the evaporator and condenser. For these experiments, the test fluid is spectroscopic grade ethanol which perfectly wetted the test loop.

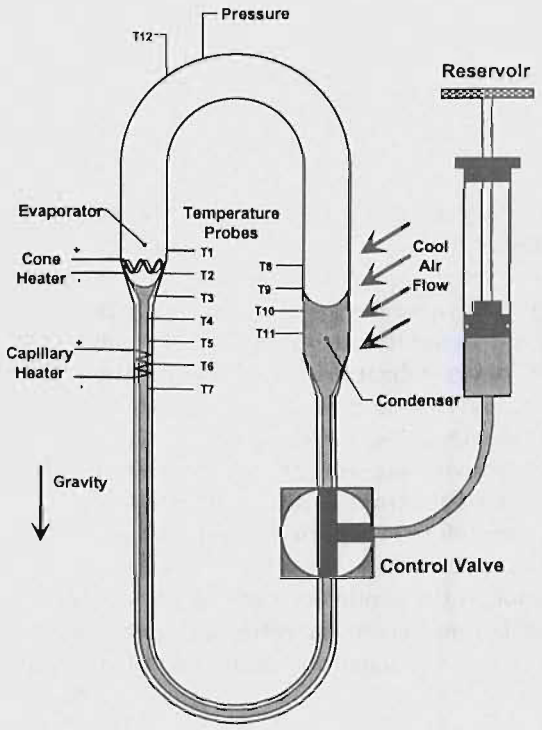

FIGURE 2. Schematic of Capillary-driven Heat Transfer (CHT) Experiment Test Loop

Heat is applied to the evaporator by either of two heaters. The first, referred to as the cone heater, is a serpentine wire attached to the conical transition section. The second, referred to as the capillary heater, is a spiral wound wire located on the capillary tubing approximately 15mm from the cone heater. When using the cone heater the wall temperature gradient along the thin film region of the meniscus is cooler towards the liquid side. The capillary heater reverses this temperature gradient. Cooling of the condenser meniscus is accomplished by forced air convection at ambient temperature. Instrumentation consists of 7 thermocouples (Type T, 40 AWG) along the length of the evaporator leg and 4 thermocouples along the length of the condenser leg. An additional thermocouple and a pressure transducer are connected to the vapor leg. The position and behavior of both the condenser meniscus and the evaporator meniscus are recorded using a single video camera.

Low gravity testing was obtained during the Microgravity Science Laboratory - 1 (MSL-1) flown on board the Space Shuttle Columbia in July, 1997. The experiment was operated in the Middeck Glovebox (MGBX) by the payload crew members. In low gravity, the test loop is filled using capillary pressure so as to allow the evaporator and condenser menisci to find a natural equilibrium position. The low gravity experiment begins with the evaporator and condenser menisci in static equilibrium as left following the filling process. Either the cone heater or the capillary heater is then set to a fixed heat input and turned on. The experiment is now monitored until evaporator dryout occurs. After evaporator dryout, the heater is turned off and the liquid in the test loop is reoriented back to the static equilibrium position. The heat input is then adjusted to the next setting and the experiment repeated.

OBSERVATIONS

One of the first experimental observations, irrespective of the gravitational environment, was the formation of a continuous liquid film over the entire length of the vapor leg. At low heat inputs the liquid film was continuous from the evaporator meniscus to the condenser meniscus. At higher heat inputs the liquid film appeared to begin slightly beyond the evaporator meniscus and extended to the condenser meniscus. This, in and of itself, is not a surprising result. However, soon after formation it became obvious that this liquid film was not stationary. Under normal gravity conditions, the liquid film would drain into the condenser meniscus and into the evaporator conical section. The latter film drainage affected the stability of the evaporating meniscus by introducing cold fluid into localized areas of the meniscus. In low gravity, the liquid film also drained, but the draining mechanism in this instance is capillarity. Variations in the capillary pressure caused the liquid film to drain and collect in the vapor leg of the test loop.

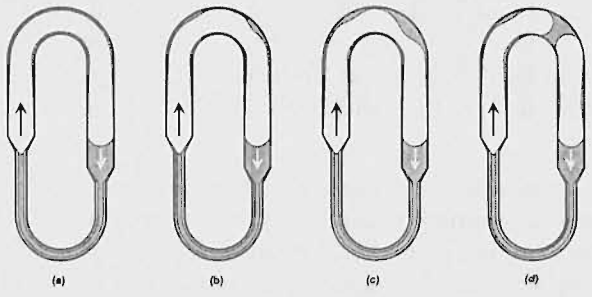

FIGURE 3. Low-Gravity Liquid Accumulation and Slug Formation in the Vapor Leg of the Test Loop

The process of the liquid pooling and eventual formation of a liquid slug in low gravity is illustrated in Figure 3. As each experiment progressed, the liquid began to pool in the outer radius of the bend in the vapor section of the test loop. This pool of liquid would grow until a slug of liquid would form, completely bridging the vapor line. The formation of this liquid slug is independent of the heat inputs. The heat input only affects the rate at which the liquid pools in the outer radius of the bend. After the formation of the liquid slug, system failure is imminent. Figures 4 and 5 show the formation of the liquid slug in the vapor leg

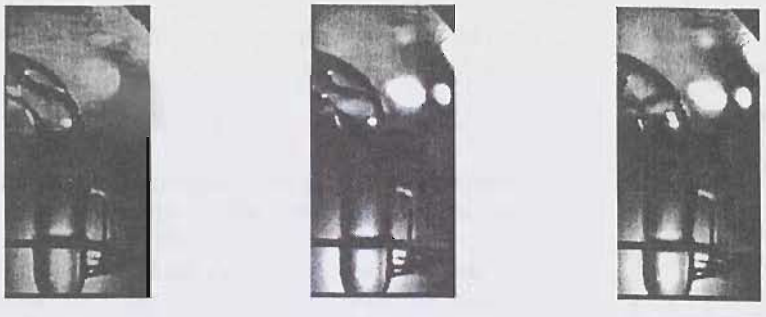

FIGURE 4. Liquid Accumulation and Formation of a Liquid Slug During a Low-Gravity Experiment

FIGURE 5. Recession of the Condenser Meniscus After Formation of a Liquid Slug in the Vapor Leg.

and the subsequent effects on the condenser meniscus during one of the low-gravity experiments. In Figure 4, the liquid film begins to pool in the outer radius of the bend region eventually bridging. Prior to complete bridging of the vapor line, there is no adverse effect on the CPL operation due to the pooling of the liquid in the bend of the vapor leg. However, after the liquid slug has formed, both vapor flow and liquid film flow to the condenser meniscus was eliminated. Subsequently, as liquid is continually fed to the evaporator,

the condenser meniscus begins to recede as shown in Figure 5. Eventually, the condenser meniscus recedes into the capillary tube thereby eliminating the pressure feeding liquid into the evaporator. At this point the evaporator dries out and the system fails.

DISCUSSION OF OBSERVATIONS

An annular liquid film inside a straight tube having a vapor core has been shown repeatedly to be fundamentally unstable to any long-wave disturbances by Gauglitz and Radke (1989), Aul and Olbricht (1990), Hu and Patankar (1994), and numerous other researchers. Such a liquid film will always breakup and form periodically spaced annular lobes or liquid slugs. In the Capillary-driven Heat Transfer (CHT) experiment, however, the formation of the liquid slug arises from a pressure gradient within the liquid film and is not due to long wavelength instabilities.

In the absence of gravity, the flow of the liquid film into the bend occurs as a result of capillary pressure differences between various regions within the tube. More appropriately, capillarity results in drainage of the annular liquid film for a low Bond number system where the Bond number is defined as $Bo = (\rho g R^2)/\sigma$. A low gravity environment is naturally a low Bond number system. The following analysis applies to small diameter tubes in normal gravity as well as large diameter tubes in low gravity.

In order to study the dynamics within the annular liquid film, four distinct regions of the film will be examined (see Figure 6). The first region (region 1) is where the liquid accumulates in the bend; that is, the outer portion of the tubing bend. Region 2 is the inside radius of the tubing bend and is located 180° from region 1 at the same centerline location (See Figure 6, section A-A). Region 3 comprises the straight portion of the vapor line. And region 4 is the condenser meniscus. Initially, the condenser meniscus is assumed to be relatively far from the bend. The liquid film will also be studied with the meniscus in the vicinity of the bend; i.e., when there is no region 3. For the purposes of this analysis the liquid film is assumed to be of uniform thickness, t. The inside diameter of the tube is $2R_i$ and the centerline radius of the bend in the tube is R_b.

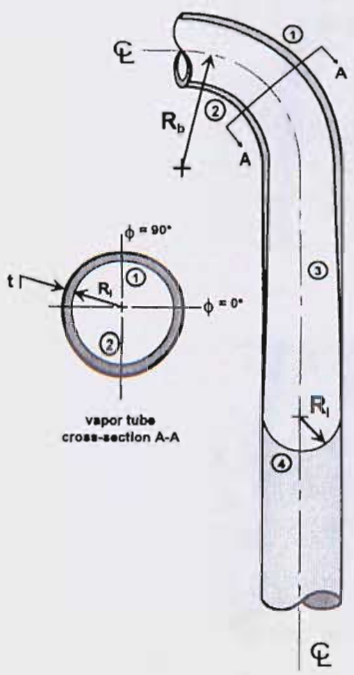

FIGURE 6. Geometry of the Annular Liquid Film

The pressure drop across a liquid-vapor interface is known from the Laplace-Young equation:

$$P_v - P_l = \sigma\left(\frac{1}{R_1} + \frac{1}{R_2}\right); \tag{1}$$

where P_v is the vapor pressure, P_l is the liquid pressure, R_1 and R_2 are the principle radii of curvature, and σ is the surface tension. One of the principle radii of curvature is the same for each of the four regions and is equal to $R_i - t$. The second principle radius curvature varies from region to region. In region 1 that radius of curvature is $R_b + (R_i - t)$. Similarly, $-[R_b - (R_i - t)]$, ∞, and $R_i - t$ are the second principle radius of curvature for regions 2, 3, and 4, respectively. In order to simplify the analysis, a film thickness ratio is defined as $\delta = t/R_i$. Also, the ratio of the radii is defined as $\Gamma = (R_i - t)/R_b$. Substituting the appropriate principle radii of curvature and the two new definitions into the Laplace-Young equation results in a set of expressions for the pressure drop across the liquid surface for each of the four regions of the liquid film.

$$\text{Region 1:} \qquad P_v - P_l|_1 = \frac{\sigma}{R_i(1-\delta)}\left[1 + \frac{\Gamma}{1+\Gamma}\right] \tag{2}$$

$$\text{Region 2:} \qquad P_v - P_l|_2 = \frac{\sigma}{R_i(1-\delta)}\left[1 - \frac{\Gamma}{1-\Gamma}\right] \tag{3}$$

$$\text{Region 3:} \qquad P_v - P_l|_3 = \frac{\sigma}{R_i(1-\delta)} \tag{4}$$

$$\text{Region 4:} \qquad P_v - P_l|_4 = \frac{2\sigma}{R_i(1-\delta)} \tag{5}$$

The interest in this study, however, is in the pressure drop within the liquid film between the four regions. The first pressure drop considered is between the inner bend radius and the outer bend radius, or from

region 2 to region 1. For an isothermal system without significant vapor flow there is no pressure drop in the vapor between regions 1 and 2. Likewise, the pressure drop in the vapor between the other regions is also assumed to be negligible. In considering a system with a condensing vapor this assumption would have to be revisited.

Now, equations 2 through 5 are rearranged so as to calculate the pressure drop within the annular liquid film between the various regions. Shown below in the left column, equations 6 through 9 describe the pressure difference within the annular liquid film when the condenser meniscus is relatively far from the tubing bend. In the right column, equations 10 through 12 describe the liquid film pressure drops for the case where the meniscus is in the vicinity of the tubing bend. In the latter case, there is no straight section (region 3) of the liquid film.

$$\Delta P_l|_{2-1} = \frac{\sigma}{R_i(1-\delta)}\left[\frac{2\Gamma}{1-\Gamma^2}\right] \quad (6)$$

$$\Delta P_l|_{3-1} = \frac{\sigma}{R_i(1-\delta)}\left[\frac{\Gamma}{1+\Gamma}\right] \quad (7)$$

$$\Delta P_l|_{2-3} = \frac{\sigma}{R_i(1-\delta)}\left[\frac{\Gamma}{1-\Gamma}\right] \quad (8)$$

$$\Delta P_l|_{3-4} = \frac{\sigma}{R_i(1-\delta)} \quad (9)$$

$$\Delta P_l|_{2-1} = \frac{\sigma}{R_i(1-\delta)}\left[\frac{2\Gamma}{1-\Gamma^2}\right] \quad (10)$$

$$\Delta P_l|_{1-4} = \frac{\sigma}{R_i(1-\delta)}\left[\frac{1}{1+\Gamma}\right] \quad (11)$$

$$\Delta P_l|_{2-4} = \frac{\sigma}{R_i(1-\delta)}\left[\frac{1}{1-\Gamma}\right] \quad (12)$$

If flow in the annular liquid film is assumed to be steady and dominated by viscous effects, then the governing equations can be reduced to the lubrication approximation and the velocity in the liquid film scales as:

$$U \sim \frac{\delta {R_i}^2}{\mu}\frac{\Delta P_l}{L}; \quad (13)$$

where L is the length scale over which the pressure difference, ΔP_l, occurs. The appropriate length scales for the pressure differences are shown in Equations 14 through 20.

$$L_{2-1} = \frac{\pi}{2}R_i(1-\delta)(2) \quad (14)$$

$$L_{3-1} = \frac{\pi}{2}R_i(1-\delta)\left[\frac{1+\Gamma}{\Gamma}\right] \quad (15)$$

$$L_{2-3} = \frac{\pi}{2}R_i(1-\delta)\left[\frac{1-\Gamma}{\Gamma}\right] \quad (16)$$

$$L_{3-4} = \frac{\pi}{2}R_i(1-\delta) \quad (17)$$

$$L_{2-1} = \frac{\pi}{2}R_i(1-\delta)(2) \quad (18)$$

$$L_{1-4} = \frac{\pi}{2}R_i(1-\delta) \quad (19)$$

$$L_{2-4} = \frac{\pi}{2}R_i(1-\delta) \quad (20)$$

The potential for liquid flow can be rewritten in terms of the Capillary number, where $Ca = \mu U\sigma$ by combining the expressions for the pressure drop in the liquid film, ΔP, the length scale associated with the pressure drop, L, and the velocity scale in the liquid film, U. When the condenser meniscus is relatively far from the tubing bend, the resulting expressions for the Capillary numbers between each of the regions are shown in Equations 21 through 24. The Capillary numbers for when the condenser meniscus is near the bend are expressed in Equations 25 through 27.

$$Ca|_{2-1} \sim \frac{2}{\pi}\left(\frac{\delta}{1-\delta}\right)^2\left[\frac{\Gamma}{1-\Gamma^2}\right] \quad (21)$$

$$Ca|_{3-1} \sim \frac{2}{\pi}\left(\frac{\delta}{1-\delta}\right)^2\left[\frac{\Gamma}{1+\Gamma}\right]^2 \quad (22)$$

$$Ca|_{2-3} \sim \frac{2}{\pi}\left(\frac{\delta}{1-\delta}\right)^2\left[\frac{\Gamma}{1-\Gamma}\right]^2 \quad (23)$$

$$Ca|_{3-4} \sim \frac{2}{\pi}\left(\frac{\delta}{1-\delta}\right)^2 \quad (24)$$

$$Ca|_{2-1} \sim \frac{2}{\pi}\left(\frac{\delta}{1-\delta}\right)^2\left[\frac{\Gamma}{1-\Gamma^2}\right] \quad (25)$$

$$Ca|_{1-4} \sim \frac{2}{\pi}\left(\frac{\delta}{1-\delta}\right)^2\left[\frac{1}{1+\Gamma}\right] \quad (26)$$

$$Ca|_{2-4} \sim \frac{2}{\pi}\left(\frac{\delta}{1-\delta}\right)^2\left[\frac{1}{1-\Gamma}\right] \quad (27)$$

During the Capillary-driven Heat Transfer (CHT) experiment, the thickness of the annular liquid film was calculated to be on the order of 250 μm. The inside diameter of the vapor leg of the test loop is

10 mm and the bend radius of the test loop is 20 mm. Therefore, for the CHT experiment the film thickness ratio, δ, is 0.05 and the radius ratio, Γ, is 0.2375. Based upon these parameters, the Capillary numbers for the CHT experiment are calculated and shown in Table 1 for both the case where the condenser meniscus is relatively far from the tubing bend and for the case where the condenser meniscus is near the tubing bend. The Capillary numbers for both positions of the condenser meniscus are

TABLE 1. Capillary Numbers for the Annular Liquid Film in the CHT Experiment

Meniscus far from bend		Meniscus near the bend	
Regions	$Ca \cdot 10^5$	Regions	$Ca \cdot 10^5$
2 - 1	44	2 - 1	44
3 - 1	7	1 - 4	142
2 - 3	17	2 - 4	231
3 - 4	176		

represented pictorially in Figure 7, where the length of the arrow representative of the magnitude of the liquid flows. In the case where the meniscus is relatively far from the tubing bend (Figure 7a), the liquid flow into the bend is much larger than the liquid flow out of the bend. Also, the liquid flow into the condenser meniscus is an order of magnitude higher than any other liquid film flows in the system. This implies that there is always significant drainage into the condenser meniscus even in low gravity systems and that the liquid will accumulate in the outer region of the tubing bend in any low Bond number system.

Similarly, for the case where the condenser meniscus is in the vicinity of the tubing bend (Figure 7b), the liquid flow into the meniscus is an order of magnitude greater than any other liquid flow in the annular film. This has the effect of draining the bend region of the tube and can prevent the formation of the liquid slug *in that location only.* The prevention of the liquid slug formation was observed during one particular run of the CHT experiment where the condenser meniscus was very near the bend. A liquid slug still formed, however, on the other side of the test loop in the evaporator section of the vapor leg.

The variation in the Capillary number between the various regions is only a function of the geometry of the system and is not a function of the properties of the liquid. Therefore, the liquid film flows illustrated in Figure 7 are typical of the flows in any annular liquid film within a bend in a low Bond number system.

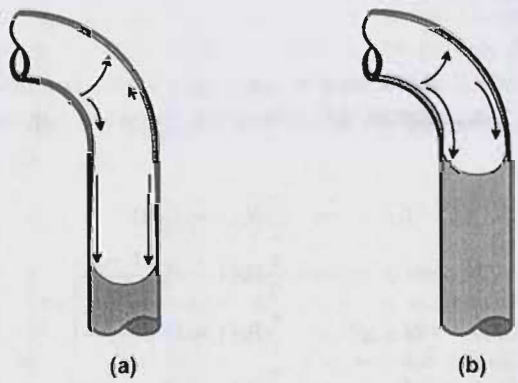

FIGURE 7. Illustration of the Direction and Relative Magnitude of Liquid Film Flows for Two Cases; (a) the Condenser Meniscus Relatively Far from the Tubing Bend and (b) the Condenser Meniscus in the Vicinity of the Tubing Bend

CONCLUSIONS

During the operation of the CHT experiment both in normal gravity and in low gravity a liquid film formed over the entire vapor leg of the loop. In normal gravity, the draining of this film affected the stability of the evaporating meniscus, but was not directly responsible for evaporator dry out. In low gravity, however, the drainage of the annular liquid film resulted in an accumulation of liquid in the outer radius of the bend in the tubing. The liquid in this region eventually bridged the vapor leg blocking the flow of vapor to the condenser meniscus. Subsequently, both condenser dryout and evaporator dryout ensued and the system failed. The flows in the annular liquid film will always collect in the bend of the tube because of capillary forces. This mode of failure was not appreciated before the on-orbit experiment. It is very probable that previous low-gravity capillary pumped loop experiments exhibited poor performance due to the formation of liquid slugs in the vapor line since all of the designs to date have incorporated a significant number of bends in the vapor leg.

Acknowledgments

The authors would like to acknowledge the support for this research from NASA Microgravity Science under grants NAG3-1391 and NAG3-1919.

References

Aul, R. W. and W. L. Olbricht (1990) "Stability of a thin annular film in pressure-driven, low-Reynolds-number flow through a capillary", in *J. Fluid Mech.*, 215:585-599.

Gauglitz, P. A. and C. J. Radke (1990) "The Dynamics of Liquid Film Breakup in Constricted Cylindrical Capillaries", in *J. Colloid Interface Sci.*, 134(1):14-40.

Hu, H. H. and N. Patankar (1994) "Non-Axisymmetric Instability of Core-Annular Flow", in *Two Fluid Flows - With or Without Phase Change*, AMD-Vol. 184, A. Narain, D. A. Siginer, and K. M. Kelkar, eds, The American Society of Mechanical Engineers, New York, presented at the 1994 International Mechanical Engineering Congress and Exposition, Chicago:33-39.

Ku, J. (1995) "Start-Up Issues of Capillary Pumped Loops", 9th International Heat Pipe Conference, Albuquerque, New Mexico.

Ku, J. , E. J. Kroliczek, M. McCabe, and S. M. Benner (1988) "A High Power Spacecraft Thermal Management System", in *AIAA Paper No. 88-2702.*

Richter, R. and J. M. Gottschlicht (1994) "Thermodynamic Aspects of Heat Pipe Operation", in *J. Thermophysics and Heat Transfer*, 8(2):334-340.

Nomenclature

L	-	length scale for ΔP
P	-	pressure
R_i	-	inside radius of tubing
R_b	-	bend radius of tubing
t	-	thickness of liquid film
U	-	liquid velocity scale
μ	-	absolute viscosity
σ	-	surface tension
δ	-	ratio of film thickness to inside radius, t/R_i
Γ	-	ratio of radii, $R_i(1-\delta)/R_b$
Bo	-	Bond Number, $\rho g R^2/\sigma$
Ca	-	Capillary number, $\mu U/\sigma$

subscripts

1	-	outer portion of the tubing bend
2	-	inner portion of the tubing bend
3	-	straight section of the tubing
4	-	condenser meniscus region
l	-	liquid
v	-	vapor